

Synthesis of a New Lipophilic Bilirubin. Conformation, Transhepatic Transport and Glucuronidation

Justin O. Brower,^a David A. Lightner^{a,*} and Antony F. McDonagh^b

^aDepartment of Chemistry, University of Nevada, Reno, NV 89557-0020, USA

^bG.I. Unit and the Liver Center, University of California, San Francisco, CA 94143-0538, USA

Received 3 July 2000; revised 4 August 2000

Abstract—Analogues of symmetrical bilirubin isomers with vinyl groups replaced by *n*-butyls (**1** and **2**) were synthesized and found to be much more soluble in nonpolar solvents than either bilirubin itself or its analogues with ethyls in place of vinyls (**3** and **4**). The increased lipophilicity of **1** and **2** allowed, for the first time, vapor pressure osmometric molecular wt. determinations of a bilirubin acid, showing in CHCl₃ solvent: MW_{obs}=632±10 for **1**, and 637±10 for **2** (both formula weight 644)—data that clearly indicate monomers and no dimers. The induced circular dichroism (ICD) spectra of **1** and **2**, with negative exciton chirality Cotton effects, are quite like those of **3** and **4** in chloroform containing quinine, but the ICDs in aqueous buffer containing human serum albumin differ considerably. Rubins **1**, **3** and **4** exhibit dissimilar but positive exciton chirality Cotton effects, while **2** shows a negative exciton chirality Cotton effect. The metabolism of the *n*-butyl rubins in the rat is highly dependent on the specific *endo* or *exo* location of the *n*-butyl groups. Rubin **2**, with two *endo n*-butyl groups was metabolized rather like the corresponding mesobilirubin (**4**) or natural bilirubin itself, being converted to a mono and diglucuronide that were excreted promptly in bile. The presence of the bulky *endo n*-butyl groups and the high lipophilicity of the compound seemed to interfere with glucuronidation in the liver only slightly. In contrast, the similar, yet even more lipophilic *n*-butyl rubin **1**, which has two *exo n*-butyl groups, was glucuronidated and excreted in bile in the rat rather poorly. © 2000 Elsevier Science Ltd. All rights reserved.

Introduction

Bilirubin (Fig. 1) is an important metabolite produced in many vertebrates, including humans.^{1,2} Because of its role in human biology, considerable effort has been directed toward understanding the relationship between its metabolism, molecular structure and chemical properties. Of special focus is its hydrophobicity and unique capacity to fold into a ridge-tile conformation³ wherein the two propionic acid side chains are linked by intramolecular hydrogen bonds to their opposing dipyrrole units (Fig. 1).^{3–8} The intramolecular hydrogen bonding depicted in Fig. 1 has several consequences: it dictates the stereochemistry of the pigment;^{3–6} it reduces the polarity of the molecule compared to analogues with propionic acids relocated away from C(8) and C(12);⁹ and it makes the compound intrinsically unexcretable *in vivo* in mammals, except by conversion to glycosyl ester conjugates.^{1,2,10} In earlier studies, we perturbed the hydrogen bonding by lengthening the propionic acid chains and learned that with intermediate length acids, e.g. pentanoic, hexanoic, heptanoic, the pigment became more polar than bilirubin (suggesting less effective hydrogen bonding).^{11,12} However,

with very long chains, e.g. undecanoic and eicosanoic acids, the pigment behaved much like a fatty acid.^{13,14} To increase the lipophilicity more modestly, we have synthesized **1** and **2** (Fig. 1), two new bilirubin analogues with *n*-butyl groups replacing vinyl groups and structurally related to mesobilirubins-III α and XIII α (**3** and **4**). In this paper, we describe the syntheses and the solution and metabolic properties of these novel hydrophobic bilirubins.

Results and Discussion

Synthesis

n-Butyl rubins **1** and **2** share a common central core containing two identical pyrrole rings. We designed their syntheses¹⁵ to make use of dipyrromethane dialdehyde **5**, which could be condensed with either **6** or **7** (Scheme 1). Synthesis of **5** proceeded smoothly from the di-carbo-*tert*-butoxy derivative **18** by reaction with TFA then triethyl orthoformate. Diester **18** was prepared in satisfactory yield by solvolysis of the acetoxymethyl monopyrrole **19**, which was prepared from **20** by reaction with Pb(OAc)₄. The synthesis of **20** followed standard Fischer–Knorr methods,^{12,15} by condensing the oxime derived from *tert*-butyl acetoacetate with methyl 4-acetyl-5-oxohexanoate (from Michael reaction between pentane-2,4-dione and methyl acrylate) with Zn in acetic acid.

Keywords: pyrroles; conformation; hydrogen-bonding; circular dichroism; liver; bile.

* Corresponding author. Tel.: +775-784-4980; fax: +775-784-6804; e-mail: lightner@unr.edu

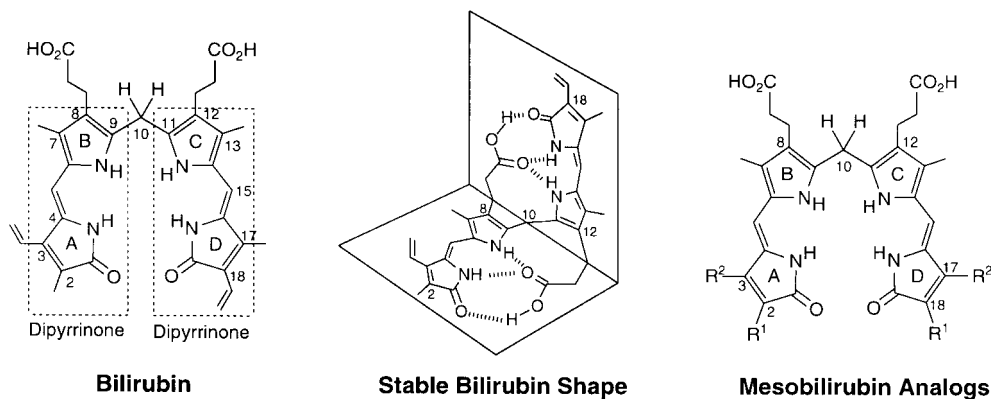
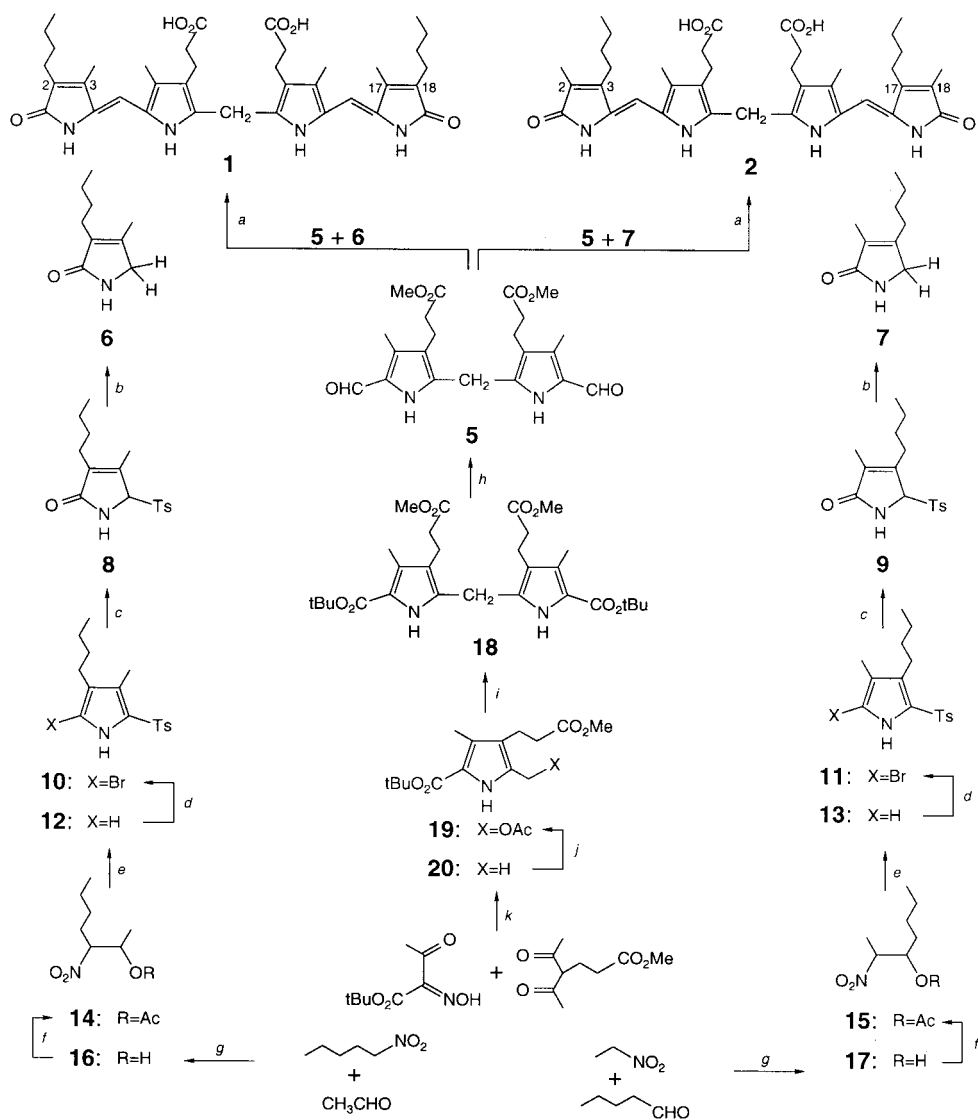


Figure 1. (Left) Bilirubin with its two dipyrinone chromophores in a porphyrin-like shape. (Center) Bilirubin in its energetically most stable, intramolecularly hydrogen-bonded ridge-tile conformation. Only one of two enantiomeric conformers is shown, and hydrogen bonds are shown by hatched lines. (Right) Mesobilirubin analogs of bilirubin. **1:** R¹=*n*-butyl, R²=methyl; **2:** R¹=methyl, R²=*n*-butyl; **3:** R¹=ethyl, R²=methyl; and **4:** R¹=methyl, R²=ethyl.



^a KOH/CH₃OH/H₂O, refl.; ^b NaBH₄/EtOH; ^c TFA, then H₂O; ^d PhNMe₃Br₃/CH₂Cl₂, 0°C; ^e TosMIC, TMG; ^f Ac₂O, DMAP; ^g KF; ^h TFA, then (EtO)₃CH; ⁱ *p*TSA/HOAc; ^j Pb(OAc)₄/HOAc, Ac₂O; ^k Zn/HOAc.

Pyrrolinones **6** and **7** were prepared by Barton–Zard pyrrole-forming reactions¹⁶ between 3-nitro-2-heptyl acetate (**14**) and *p*-toluenesulfonylmethyl isocyanide (TosMIC) to give **12** in 65% yield, or between 3-nitro-2-heptyl acetate (**15**) and TosMIC to give **13** in 75% yield. The isomeric nitroheptyl acetates were prepared by standard acetylation methods from the corresponding nitroheptanols, which were prepared by Henry reactions—**16** in 83% yield from reaction of 1-nitropentane and acetaldehyde using KF as base; **17** in 82% yield from reaction of nitroethane and valeraldehyde. Tosyl pyrroles **12** and **13** were converted to pyrrolinones **6** and **7**, respectively, by a similar sequence of reactions. Thus, bromination of **12** with phenyltrimethylammonium tribromide gave **10** in 97% yield, while the same reaction converted **13** to **11** quantitatively. Treatment of **10** in TFA then water gave tosylpyrrolinone **8** in 68% yield, and similar treatment of **11** gave **9** in 36% yield. The tosyl groups of **8** and **9** were removed by reduction with sodium borohydride in ethanol, affording **6** and **7**, respectively, in 90 and 74% yields.

Reaction of **5** with excess **6** in refluxing aqueous methanolic potassium hydroxide afforded **1** as a bright yellow solid in 43% yield. Similarly, reaction of **5** with **7** gave **2** in 40% yield.

Solution properties

The limited solubilities of bilirubin (Fig. 1) and its hydrogenated analogs, mesobilirubins **3** and **4**, have precluded measurements of their molecular weights in solution. In **1** and **2** the *n*-butyl substituents increase the solubility of the pigments in chloroform sufficiently for the reliable determination of molecular weight by vapor pressure osmometry. Their molecular weights were thus determined to be 632 ± 10 (for **1**) and 637 ± 10 (for **2**) in the concentration range $1.6\text{--}5.6 \times 10^{-3}$ M. Since the formula weights are 644 g/mol, **1** and **2** are clearly monomeric in chloroform.

Substituting *n*-butyl groups for the ethyls of the parent mesobilirubin analogs (**3** and **4**) leads to longer retention times for **1** and **2** (cf. **1**: 29.8 min; **2**: 26.0 min; **3**: 16.4 min; **4**: 15.4 min) on reverse-phase HPLC, suggesting that **1** and **2** are considerably more lipophilic than their ethyl analogs. Similarly, on silica gel TLC using 1% CH₃OH in CH₂Cl₂ eluent, **1** (*R_f* 0.76) moves faster than **2** (*R_f* 0.64), and **3** (*R_f* 0.69) moves faster than **4** (*R_f* 0.57). However, **3** moves faster than **2**, suggesting that the presence of the larger group at the *exo* position on the lactam rings shields the polar lactam group from the silica surface more effectively than an *exo* methyl group.

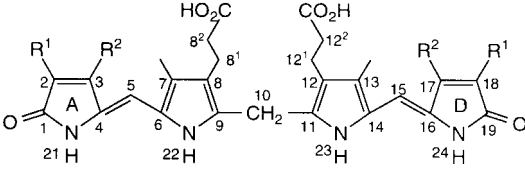
¹³C NMR and structure

The constitutional structures of mesobilirubins-III α and XIII α (**3** and **4**) are well established.^{9,12,17} The structure of **1** is rather similar to **3**, differing only in the *exo* position substituents, while the structures of **2** and **4** differ only in the *endo* substituents. Thus, the ¹³C NMR spectral data (Table 1) of **1–3** follow the same trends reported previously for **4**.^{9,12} Ring carbons 2 and 18 of **1** and **3** are more deshielded than those of ring carbons 3 and 17, but in **2** and **4** the

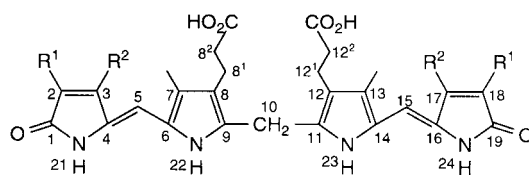
reverse obtains—according to the *exo* or *endo* location of the larger alkyl group. In contrast, ring carbons 4/16, 6/4, 7/13, 8/12 and 9/11 do not show a similar sensitivity. Nor do bridging carbons 5/15 and 10. Although the chemical shifts of the methyl groups at 2/18 or 3/17 do not show any remarkable sensitivity to the *exo* vs *endo* location of the larger β -alkyl substituent on rings A and D, the 7/13-methyls are significantly more deshielded when the ethyl or *n*-butyl substituents are located on (*exo*) ring carbons 2 and 18 than on (*endo*) 3 and 17.

Many of the general ¹³C trends that distinguish the ¹³C NMR spectra of **1** and **3** from **2** and **4** in CDCl₃ can also be found in (CD₃)₂SO (Table 1), particularly the distinctions in the lactam ring carbons 2 and 18 vs 3 and 17, and the methyls at C(7) and C(13). Certain general trends also distinguish ¹³C NMR resonances obtained in CHCl₃ from those in (CD₃)₂SO, especially the 1 ppm deshielding of the lactam

Table 1. Comparison of ¹³C NMR chemical shift assignments for *n*-butyl mesobilirubin analogs **1** (R¹=*n*-Bu, R²=Me) and **2** (R¹=Me, R²=*n*-Bu) with **3** (R¹=Et, R²=Me) and **4** (R¹=Me, R²=Et) in (CD₃)₂SO and in CDCl₃ (chemical shifts in δ (ppm) downfield from (CH₃)₄Si)



Position	1	2	3	4
1,19-CO	174.01 174.98	173.99 175.11	171.55 174.85	171.92 175.12
2,18	128.11 129.77	123.46 124.15	129.07 129.77	122.89 123.89
2,18-CH ₃ (or 3,17)-CH ₃	9.45 10.31	9.10 10.27	9.28 10.30	9.15 10.31
3 ¹ ,17 ¹ (or 2 ¹ ,18 ¹)-CH ₂	22.02 25.36	23.23 24.50	16.33 16.85	17.15 18.06
3 ² ,17 ² (or 2 ² ,18 ²)	30.68 31.33	32.08 32.77	13.49 13.70	14.82 15.11
3 ³ ,17 ³ (or 2 ³ ,18 ³)-CH ₂	22.72 22.81	21.93 22.77	–	–
3 ⁴ ,17 ⁴ (or 2 ⁴ ,18 ⁴)-CH ₃	13.78 14.13	13.75 14.06	–	–
3,17	141.36 142.43	145.76 147.31	140.92 142.01	147.14 148.59
4,16	129.12 128.97	128.30 129.20	129.38 130.21	127.78 128.59
5,15-CH=	97.96 100.77	97.82 100.89	98.01 100.84	97.70 100.74
6,14	121.98 123.80	122.47 123.86	121.95 123.82	122.43 123.57
7,13	122.50 124.37	121.95 124.47	122.51 124.38	121.98 124.36
7,13-CH ₃	9.12 9.91	8.30 8.10	9.12 9.73	8.07 8.18
8,12	119.23 119.58	119.25 119.72	119.23 119.59	119.26 119.64
8 ¹ ,12 ¹ -CH ₂	19.25 18.79	19.25 18.83	19.25 18.78	19.23 18.76
8 ² ,12 ² -CH ₂	34.35 32.88	34.35 32.92	34.32 32.87	34.56 32.87
8 ³ ,12 ³ -COOH	171.71 179.73	171.88 179.74	173.99 179.99	174.12 179.72
9,11	130.27 133.32	130.33 133.42	130.28 133.34	130.38 133.39
10-CH ₂	23.71 22.45	23.42 22.50	23.54 22.45	23.34 22.44

Table 2. ¹H NMR chemical shift assignments for *n*-butyl mesobilirubin analogs **1** (R¹=*n*-Bu, R²=Me) and **2** (R¹=Me, R²=*n*-Bu) with **3** (R¹=Et, R²=Me) and **4** (R¹=Me, R²=Et) in (CD₃)₂SO and in CDCl₃ (chemical shifts in δ (ppm) downfield from (CH₃)₄Si; US denotes signal obscured by solvent)

Position	1	2	3	4
α,α'-COOH	11.92 13.65	11.92 13.65	11.89 <i>Not Seen</i>	11.89 13.64
21,24-NHCO	9.76 10.60	9.80 10.59	9.74 10.59	9.77 10.58
22,23-NH	10.31 9.16	10.32 9.15	10.31 9.16	10.31 9.15
2,18-CH ₃ (or 3,17)-CH ₃	2.00 2.06	1.77 1.86	2.00 2.07	1.78 1.86
3 ¹ ,17 ¹ (or 2 ¹ ,18 ¹)-CH ₂	2.23 ^a 2.29 ^b	2.47 ^f 2.46 ^m	2.25 ^t 2.32 ^t	US 2.48
3 ² ,17 ² (or 2 ² ,18 ²)	1.39 ^c 1.44 ^c	1.46 ^c 1.48 ^c	1.01 ^l 1.06 ^l	1.01 ^l 1.12 ^u
3 ³ ,17 ³ (or 2 ³ ,18 ³)-CH ₂	1.27 ^c 1.30 ^c	1.33 1.34 ^c	– –	– –
3 ⁴ ,17 ⁴ (or 2 ⁴ ,18 ⁴)-CH ₃	0.88 ^d 0.89 ^c	0.91 ^f 0.91 ^f	– –	– –
5,15-CH=	5.99 6.03	5.93 6.04	5.94 6.04	5.95 6.05
7,13-CH ₃	2.06 2.15	1.99 2.15	2.07 2.16	2.00 2.16
8 ¹ ,12 ¹ -CH ₂	2.41 ^f 3.01 ^{g,h,i} 2.56 ^{j,k}	2.42 ⁿ 3.01 ^{h,o,p} 2.56 ^{p,q,r}	2.41 ^u 3.01 ^{v,w,x} 2.59 ^{x,y,z}	2.43 ^{bb} 3.01 ^{v,w,x} 2.57 ^{x,y,z}
8 ² ,12 ² -CH ₂	1.96 ^f 2.88 ^{g,i,l} 2.79 ^{j,k,l}	1.98 ⁿ 2.88 ^{g,q,s} 2.79 ^{h,r,s}	1.96 ^u 2.88 ^{v,y,aa} 2.82 ^{w,zaa}	1.98 ^{bb} 2.88 ^{v,y,aa} 2.80 ^{w,zaa}
10-CH ₂	3.95 4.06	3.95 4.07	3.96 4.07	3.96 4.08

^a t, *J*=7.1 Hz.^{aa} *J*=–18.7 Hz.^b t, *J*=7.6 Hz.^{bb} t, *J*=8.0 Hz.^c m.^d t, *J*=7.0 Hz.^e t, *J*=7.4 Hz.^f t, *J*=7.3 Hz.^g *J*=14.8 Hz.^h *J*=2.7 Hz.ⁱ *J*=–16.6 Hz.^j *J*=2.3 Hz.^k *J*=3.4 Hz.^l *J*=–19.1 Hz.^m t, *J*=7.5 Hz.ⁿ t, *J*=8.1 Hz.^o *J*=14.5 Hz.^p *J*=–14.8 Hz.^q *J*=2.6 Hz.^r *J*=3.7 Hz.^s *J*=–18.6 Hz.^t *J*=7.5 Hz.^u t, *J*=7.5 Hz.^v *J*=12.7 Hz.^w *J*=3.0 Hz.^x *J*=–14.7 Hz.^y *J*=2.6 Hz.^z *J*=3.3 Hz.

carbonyl carbon (1,19-C=O), the 10-CH₂ and the 5,15-CH= in CDCl₃ and the 6–8 ppm deshielding of the carboxylic acid carbon.

Analysis of hydrogen bonding and conformation by ¹H NMR

As may be recognized from their structures, bilirubin and mesobilirubins **1–4** each comprise two dipyrinone units (Fig. 1), which participate avidly in intramolecular hydrogen bonding.^{4,18,21} Hydrogen bonding strongly perturbs dipyrinone lactam and pyrrole N–H chemical shifts (~7.5 and 8 ppm, respectively, in monomers), causing large deshieldings (~11 and 10 ppm, respectively) in intermolecularly hydrogen-bonded dipyrinone–dipyrinone dimers in CDCl₃.^{18,19} In bilirubins, dipyrinone N–H chemical shifts have been used to detect and distinguish dipyrinone–dipyrinone intermolecular hydrogen bonding^{7,20–25} and dipyrinone–carboxylic acid intramolecular hydrogen bonding.^{6,7,26–28} Such ¹H NMR studies showed that the pyrrole N–H chemical shift of

bilirubin and mesobilirubin is ~9.2 ppm in CDCl₃ when the dipyrinone and carboxylic acid groups are linked by intramolecular hydrogen bonding. The pyrrole N–H is shielded by ~1 ppm relative to that found in a planar dipyrinone dimer.^{18,19} Such shielding correlates with a ridge-tile shape (Fig. 1) wherein the pyrrole N–H lies above the opposing pyrrole or dipyrinone π-system. Consequently, NH chemical shifts have proven to be an excellent probe of hydrogen bonding involving dipyrinones and rubin stereochemistry.

In Table 2, the ~9.15 ppm chemical shift of the pyrrole N–H in **1–4** in CDCl₃ is consistent with acid to dipyrinone intramolecular hydrogen bonding of the type shown in Fig. 1. In (CD₃)₂SO, which is thought to interpose solvent molecules into the bilirubin hydrogen bonding matrix,^{7,8,29,30} the CO₂H and lactam N–H signals become more shielded than in CDCl₃, but the pyrrole N–H typically becomes more deshielded, an indication possibly of a conformational change that repositions the N–H.

Table 3. ^1H NMR chemical shifts (δ , ppm downfield from $(\text{CH}_3)_4\text{Si}$) and coupling constants (J in Hertz from 500 MHz spectra) for the propionic acid $\text{C}_\beta\text{H}_\text{A}\text{H}_\text{X}-\text{C}_\alpha\text{H}_\text{B}\text{H}_\text{C}-\text{CO}_2\text{H}$ segments of **1–4** in CDCl_3 at 22°C

MBR	$\beta\text{-CH}_2$		$\alpha\text{-CH}_2$		MBR	$\beta\text{-CH}_2$		$\alpha\text{-CH}_2$	
	H_X	H_A	H_B	H_C		H_X	H_A	H_B	H_C
1 δ :	3.01	2.56	2.79	2.88	3 δ :	3.01	2.59	2.82	2.88
	$J_{\text{BX}}=14.80$	$J_{\text{AB}}=2.30$	$J_{\text{AB}}=2.30$	$J_{\text{AC}}=14.50$		$J_{\text{BX}}=12.70$	$J_{\text{AB}}=2.60$	$J_{\text{AB}}=3.00$	$J_{\text{AB}}=12.70$
	$J_{\text{CX}}=2.70$	$J_{\text{AC}}=3.40$	$J_{\text{BX}}=3.40$	$J_{\text{CX}}=2.70$		$J_{\text{CX}}=3.00$	$J_{\text{AC}}=3.30$	$J_{\text{BX}}=3.30$	$J_{\text{CX}}=2.60$
	$J_{\text{AX}}=-16.60$	$J_{\text{AX}}=-16.60$	$J_{\text{BC}}=-19.10$	$J_{\text{BC}}=-19.10$		$J_{\text{AX}}=-14.70$	$J_{\text{AX}}=-14.70$	$J_{\text{BC}}=-18.70$	$J_{\text{BC}}=-18.70$
2 δ :	3.01	2.56	2.79	2.88	4 δ :	3.01	2.57	2.80	2.88
	$J_{\text{BX}}=14.50$	$J_{\text{AB}}=2.60$	$J_{\text{AB}}=2.70$	$J_{\text{AC}}=14.50$		$J_{\text{BX}}=12.70$	$J_{\text{AB}}=2.60$	$J_{\text{AB}}=3.00$	$J_{\text{AC}}=12.70$
	$J_{\text{CX}}=2.70$	$J_{\text{AC}}=3.70$	$J_{\text{BX}}=3.70$	$J_{\text{CX}}=2.70$		$J_{\text{CX}}=3.00$	$J_{\text{AC}}=3.30$	$J_{\text{BX}}=3.30$	$J_{\text{CX}}=2.60$
	$J_{\text{AX}}=-14.80$	$J_{\text{AX}}=-14.80$	$J_{\text{BC}}=-18.60$	$J_{\text{BC}}=-18.60$		$J_{\text{AX}}=-14.70$	$J_{\text{AX}}=-14.70$	$J_{\text{BC}}=-18.70$	$J_{\text{BC}}=-18.70$

Further evidence for intramolecular hydrogen bonding between propionic acid and dipyrinone groups in the mesobilirubins can be elicited from an examination of vicinal coupling constants. In CDCl_3 solvent, the well-defined ABCX (ddd) coupling pattern is characteristic of restricted mobility^{6–8,26} in the $-\text{CH}_\text{A}\text{H}_\text{X}\text{CH}_\text{B}\text{H}_\text{C}-\text{COOH}$ segment which is constrained to adopt a fixed staggered geometry (Table 3) due to strong intramolecular hydrogen bonding. Analysis of the vicinal H|H coupling constants in the propionic acid chains (Table 3) clearly shows the ABCX pattern of the fixed staggered propionic acid geometry in **1–4**, thus providing strong supporting experimental evidence for folded ridge-tile structures. On the other hand, the less complicated A_2B_2 pattern found in $(\text{CD}_3)_2\text{SO}$ solvent (Table 2) indicates more motional freedom in the propionic acid segment, whose CO_2H groups are thought to be linked to the dipyrinones via bound solvent molecules.^{7,8,29,30}

The stereochemical conclusions reached above were confirmed by $^1\text{H}\{^1\text{H}\}$ -homonuclear Overhauser effect (NOE) measurements in CDCl_3 (Fig. 2). A *syn-Z*-dipyrinone conformation is confirmed by moderately strong NOEs between: (i) the pyrrole and lactam NHs within individual dipyrinones; and (ii) the vinylic hydrogens at C(5) and C(15) and the pyrrole methyls at C(7) and C(13), and the lactam methyls at C(3) and C(17). Significantly, NOEs are observed between CO_2H and lactam NH, as anticipated from intramolecularly hydrogen-bonded conformations. Taken collectively, the NMR data support intramolecularly

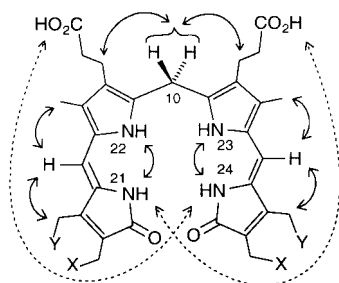


Figure 2. $^1\text{H}\{^1\text{H}\}$ -homonuclear Overhauser effects (NOEs) found in **1** ($\text{X}=\text{Pr}$, $\text{Y}=\text{H}$) and **2** ($\text{X}=\text{H}$, $\text{Y}=\text{Pr}$) and their parents **3** ($\text{X}=\text{Me}$, $\text{Y}=\text{H}$) and **4** ($\text{X}=\text{H}$, $\text{Y}=\text{Me}$), in CDCl_3 are shown by solid, double-headed curved arrows. Significant, albeit weak, NOEs are found between the CO_2H protons and the lactam N–H protons at N(21) and N(24), as indicated by dashed arrows.

hydrogen-bonded ridge-tiles for **1–4** (Fig. 3) and a fixed staggered conformation of the propionic acid segments.

UV–visible spectral analysis

The UV–visible spectra of **1–4** in a wide range of solvents of different polarity and hydrogen bonding ability are similar (Table 4). This is consistent with a single favored conformation, the ridge-tile.⁴ The UV–visible spectra of **1–4** in polar solvents invariably show λ^{max} near 430 nm and a shoulder near 395 nm. (In nonpolar solvents the shoulder lies near 420 nm.) This band shape is due to two exciton components originating in an electric transition dipole–dipole interaction between the two proximal dipyrinone chromophores oriented at a 90° angle (as in Fig. 3).⁴ The data are consistent with the ridge-tile conformation for **1–4** derived from NMR studies and support the following conformational analysis by circular dichroism spectroscopy.

Induced circular dichroism and conformation

Stereochemical investigations of bilirubin and its analogs have repeatedly indicated that: (i) the most stable conformation is one where the two dipyrinones are rotated into a ridge-tile shape; (ii) considerable stabilization of the ridge-tile is achieved by intramolecular hydrogen bonding; and (iii) the pigment adopts either of two interconverting enantiomeric ridge-tiles, as depicted in Fig. 3.^{4,8,26–28,31} The component dipyrinone chromophores of **1–4** have strongly allowed long-wavelength electronic transitions (Table 4), making them excellent candidates for transition dipole–dipole (Fig. 3) interaction (exciton coupling).^{31,32} Such intramolecular exciton interaction or resonance splitting produces two long wavelength transitions in the UV–visible spectrum and two corresponding but oppositely signed bands in the CD spectrum. According to exciton chirality theory,³³ a long-wavelength negative and short-wavelength positive CD couplet exhibits negative exciton chirality and corresponds to a negative helical disposition of the relevant dipyrinone long-wavelength transition dipoles. Usually this corresponds to the *M*-helical enantiomeric type of Fig. 3.^{4,31} But, as has been shown previously,³⁴ opening of the interplanar angle of either enantiomer without inverting molecular helicity also can cause the transition moments to invert helicity and invert the Cotton effect signs of the CD couplet.

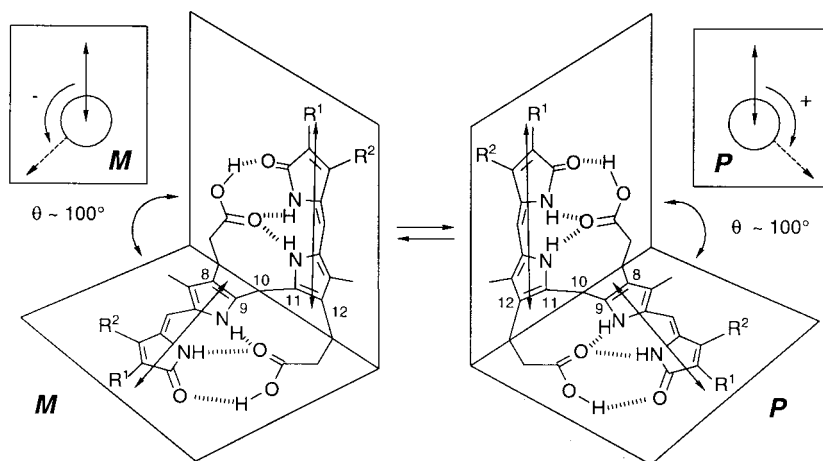


Figure 3. Interconverting intramolecularly hydrogen-bonded enantiomeric conformers of mesobilirubins **1–4** and bilirubin (see Fig. 1). The double-headed arrows represent the dipyrinone long wavelength electric transition moments (dipoles). The relative helicities (*M*, minus or *P*, plus) of the vectors are shown (inset) for each enantiomer. Hydrogen bonds are shown by hatched lines.

Table 4. Solvent-dependence of UV–visible spectral data of rubins **1–4** (at 22°C in concentrations $\sim 1.4 \times 10^{-5}$ M)

Rubin	$\Delta\epsilon^{\max}$ (λ^{\max} , nm)					
	Benzene	CHCl_3	$(\text{CH}_3)_2\text{CO}$	CH_3OH	CH_3CN	$(\text{CH}_3)_2\text{SO}$
1	61,300(436)	60,800(434)	62,300(430)	55,800(427)	59,600(426)	67,000(430)
	56,000(423) ^s	58,700(424) ^s	60,200(421) ^s	46,700(400) ^s	57,900(418) ^s	52,100(397) ^s
2	56,600(435)	55,500(434)	55,100(428)	55,100(428)	55,000(426)	63,100(430)
	51,400(419) ^s	54,100(424) ^s	54,900(422) ^s	45,600(401) ^s	52,700(416) ^s	50,500(400) ^s
3	59,800(435)	59,100(433)	56,800(426)	52,200(426)	56,700(426)	63,200(427)
	55,700(422) ^s	57,100(424) ^s	55,600(422) ^s	45,600(401) ^s	55,700(422) ^s	51,900(397) ^s
4	55,900(433)	55,400(431)	55,000(424)	52,100(427)	56,400(420)	59,100(428)
	51,600(418) ^s	53,400(418) ^s	51,800(422) ^s	45,600(403) ^s	48,900(396) ^s	50,000(401) ^s

^s Shoulders (or) inflections were determined by first and second derivative spectra.

In a nonpolar, aprotic solvent such as chloroform, the conformational equilibrium between bilirubin enantiomers can be displaced from 1:1 by adding a chiral recognition agent.^{31,35} This leads typically to an intense bisignate induced circular dichroism (ICD) Cotton effect, as has been noted previously for bilirubin in aqueous buffers with added albumin³⁶ and in chloroform with added quinine³¹ or other optically active amines.³⁵ Similarly, for the mesobilirubins of this work, in CHCl_3 strong, negative exciton chirality ICDs are observed in the presence of quinine (Fig. 4), as is characteristic of an exciton system in which the two dipyrinone chromophores of the bichromophoric rubin molecule interact by coupling locally excited $\pi \rightarrow \pi^*$ transitions (electric dipole transition moment coupling). At a molar ratio of alkaloid: pigment of $\sim 300:1$, the Cotton effect intensities reach a maximum for **3**, giving an intense bisignate CD ($\Delta\epsilon_{430}^{\max} -85$, $\Delta\epsilon_{386}^{\max} +46$), of exactly the same signed order but larger magnitudes than those seen for bilirubin or **4**.³¹ The Cotton effect intensities of **2** are nearly identical to those of its counterpart, **4**, while those of **1** are somewhat smaller than those of **3**. Interestingly, the presence of the larger alkyl group (*n*-Bu or Et) in the *exo* positions leads to more intense Cotton effects (**1** and **3**) than when they are located at the *endo* sites (**2** and **4**) (Table 5). Whether this reflects ineffective complexation/recognition or an altered pigment conformation is not immediately clear, but the presence of the larger alkyl substituent nearer the lactam carbonyl leads to larger

ICDs and perhaps promotes stronger complexation with quinine.

When human serum albumin (HSA) is used as the chiral complexation agent,³⁶ aqueous buffered (pH 7.4 Tris)

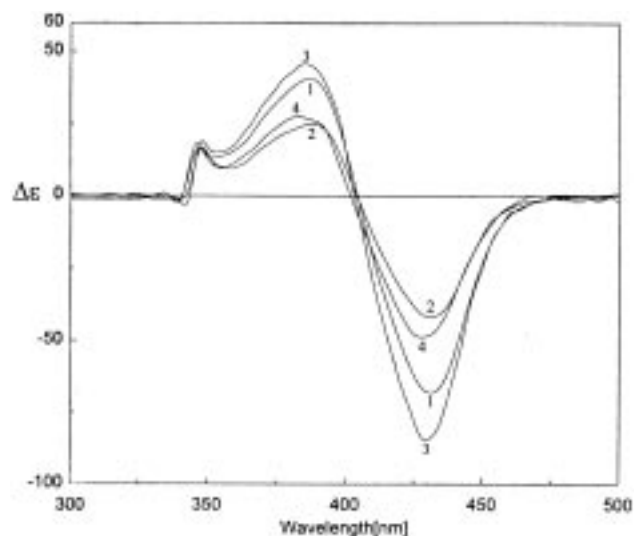


Figure 4. Circular dichroism spectra of 1.4×10^{-5} M **1–4** in CHCl_3 in the presence of ca. 4.2×10^{-3} M quinine at 22°C. The compound numbers are indicated on each CD curve.

Table 5. Comparison of circular dichroism and UV–visible spectroscopic data for **1–4** in CHCl_3 solutions containing quinine (pigment conc. $\sim 1.4 \times 10^{-5}$ M; quinine conc. $\sim 4.2 \times 10^{-3}$ M; pigment:quinine molar ratio $\sim 1:300$)

Pigment	CD			UV	
	$\Delta\epsilon^{\max}(\lambda)_1$	λ_2 at $\Delta\epsilon=0$	$\Delta\epsilon^{\max}(\lambda)_3$	ϵ^{\max}	λ (nm)
1	+41 (387)	404	-68 (431)	56,770	433
2	+25 (389)	404	-42 (431)	52,210	433
3	+46 (386)	403	-85 (430)	59,550	432
4	+27 (383)	402	-49 (428)	54,130	429

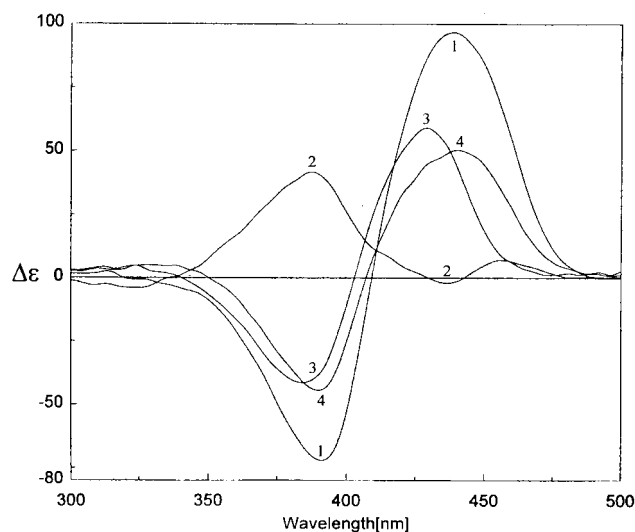


Figure 5. Circular dichroism spectra of 1.41×10^{-5} M **1**, **2**, **3** and **4** in the presence of ca. 2.8×10^{-5} M HSA in pH 7.4 Tris buffer at 22°C . The compound numbers are indicated on each CD curve.

solutions of **1**, **3** and **4** exhibit strong positive chirality bisignate ICD Cotton effects, as observed for bilirubin.³⁶ In contrast, **2** exhibits a much weaker Cotton effect that is not evidently bisignate (Fig. 5). The CD intensities of **1** are

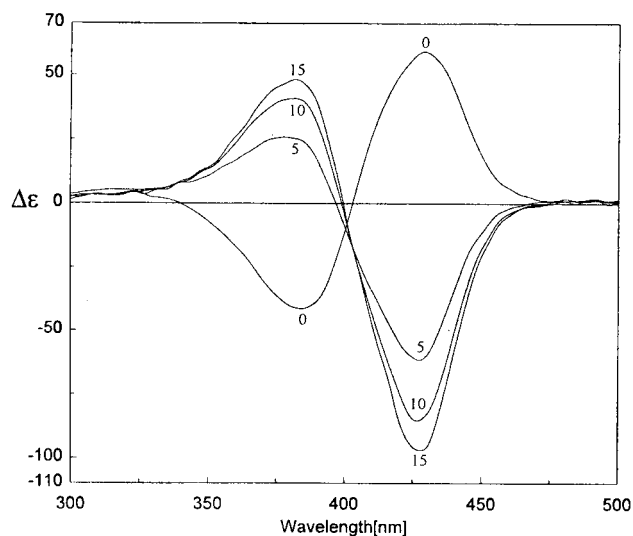


Figure 6. Circular dichroism spectra of 1.43×10^{-5} M **3** in the presence of 2.90×10^{-5} M HSA in pH 7.4 Tris buffer at 22°C , with the addition of CHCl_3 . The amounts of CHCl_3 added, $\mu\text{L}/5$ mL buffered pigment-albumin solutions, are indicated on each CD curve (μL).

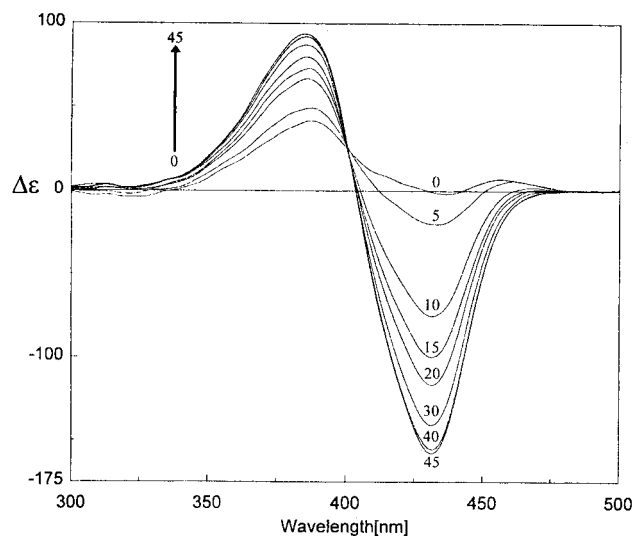


Figure 7. Circular dichroism spectra of 1.47×10^{-5} M **2** in the presence of 2.86×10^{-5} M HSA in pH 7.4 Tris buffer at 22°C , with the addition of CHCl_3 . The amounts of CHCl_3 added, $\mu\text{L}/5$ mL buffered pigment-albumin solutions, are indicated on each CD curve (μL).

nearly a third larger than those of **3** and **4**, apparently due to greater enantioselective chiral complexation by HSA for **1**. Interestingly, **3** gives more intense Cotton effects than **4**, again suggesting the importance of the larger *exo* alkyl groups for a favorable binding interaction with the chiral complexation agent. The ICD data for **1**, **3** and **4** suggest rather similar conformations on HSA; whereas, the contrasting ICD data for **2** suggest a different conformation or a mixture of conformations.

Adding trace amounts of CHCl_3 ($\mu\text{L}/\text{mL}$) to buffered aqueous HSA solutions of **1**, **2**, **3** and **4** leads to inversion of the Cotton effect signs (Figs. 6–9), as noted previously for bilirubin.³⁴ The Cotton effects of **3** (Fig. 6) invert upon addition of 5 μL CHCl_3 , and **2** immediately exhibits a

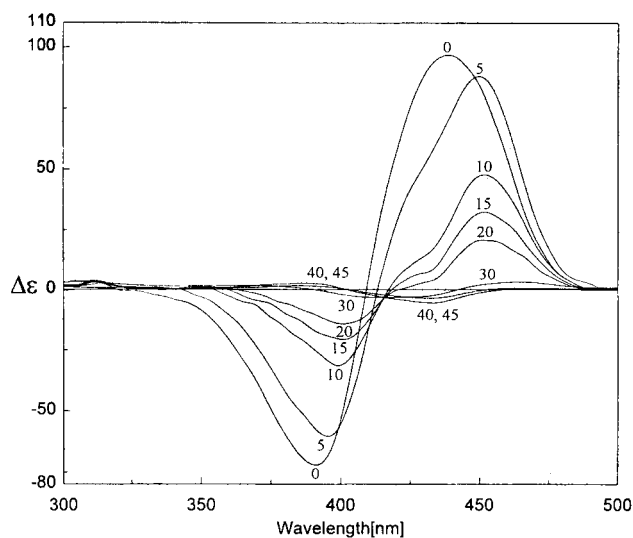


Figure 8. Circular dichroism spectra of 1.42×10^{-5} M **1** in the presence of 2.84×10^{-5} M HSA in pH 7.4 Tris buffer at 22°C , with the addition of CHCl_3 . The amounts of CHCl_3 added, $\mu\text{L}/5$ mL buffered pigment-albumin solutions, are indicated on each CD curve (μL).

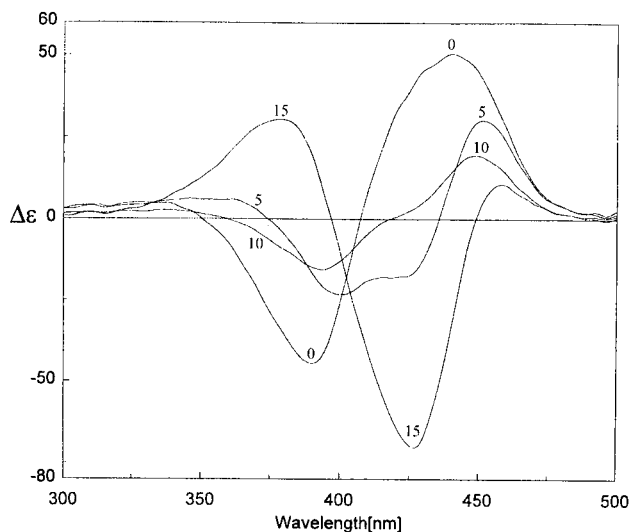


Figure 9. Circular dichroism spectra of 1.40×10^{-5} M **4** in the presence of 2.80×10^{-5} M HSA in pH 7.4 Tris buffer at 22°C, with the addition of CHCl_3 . The amounts of CHCl_3 added, $\mu\text{L}/5$ mL buffered pigment-albumin solutions, are indicated on each CD curve (μL).

negative exciton chirality (Fig. 7); whereas, for **1** (Fig. 8) and **4** (Fig. 9), the intensities are only reduced and no sign inversion occurs. Addition of a second 5 μL aliquot of CHCl_3 inverts the Cotton effect signs of **4** (but not **1**) and leads to increased magnitudes for **2** and **3**. At a total of 15 $\mu\text{L}/5$ mL, the solutions containing **3** and **4** are saturated, and very intense bisignate Cotton effects are seen for **2** and **3**, but the Cotton effects of **1** are still not inverted. Solutions of **1** and **2** are able to dissolve more CHCl_3 , again indicating the importance of the large lipophilic *n*-butyl groups. Addition of 40–45 μL of CHCl_3 causes the bisignate CD of **2** to reach its maximum values (Table 6). Rubin **1** behaves rather differently. Added CHCl_3 causes a diminution of the Cotton effect intensities, eventually to zero, and only weakly inverted Cotton effects are seen after addition of 40–45 μL of CHCl_3 . The initially large Cotton effects of **1** on HSA and their resistance to inversion with added CHCl_3 is remarkable and suggest that **1** is tightly bound to HSA in a favorable binding site. Apparently it is the location (*exo*) of the *n*-butyl groups rather than their presence that is responsible for the phenomenon.

Table 6. Influence of chloroform on the circular dichroism spectra for **1–4** (chloroform was added to 5 mL solutions that were $\sim 1.4 \times 10^{-5}$ M in pigment and had a 1:2 molar ratio of pigment to HSA (human serum albumin) at 22°C in pH 7.4 Tris buffer containing HSA)

Pigment	CHCl_3 (μL)	CD			UV	
		$\Delta\epsilon^{\max}(\lambda)_1$	λ_2 at $\Delta\epsilon=0$	$\Delta\epsilon^{\max}(\lambda)_3$	ϵ^{\max}	λ (nm)
1	0 μL	-72 (391)	409	+97 (439)	48,400	409
2		+37 (388)	435	+7 (456)	51,200	437
3		-41 (384)	403	+59 (429)	54,300	434
4		-44 (390)	407	+50 (440)	44,800	434
1	5 μL	-60 (396)	413	+88 (450)	49,600	408
2		+49 (388)	412	-20 (433)	49,200	435
3		+26 (378)	399	-85 (427)	52,100	429
4		-23 (400)	418	+19 (449)	44,500	431
1	10 μL	-31 (399)	417	+48 (452)	48,300	410
2		+67 (388)	405	-75 (431)	55,900	435
3		+41 (382)	399	-85 (427)	52,100	429
4		-16 (394)	418	-19 (449)	46,500	431
1	15 μL	-21 (401)	418	+32 (452)	46,500	412
2		+73 (387)	404	-100 (431)	59,500	434
3		+48 (382)	399	-97 (428)	48,600	429
4		+30 (378)	397	-70 (427)	47,100	431
1	20 μL	-14 (401)	421	+21 (451)	42,100	421
2		+78 (386)	404	-117 (431)	50,600	433
3		*	*	*	*	*
4		*	*	*	*	*
1	30 μL	-3 (413)	441	+4 (464)	40,500	423
2		+87 (386)	403	-141 (431)	50,900	433
3		*	*	*	*	*
4		*	*	*	*	*
1	40 μL	+2 (384)	402	-4 (432)	38,900	424
2		+94 (385)	403	-158 (431)	50,900	433
3		*	*	*	*	*
4		*	*	*	*	*
1	45 μL	+3 (386)	403	-6 (433)	38,300	424
2		+92 (386)	403	-156 (432)	49,800	433
3		*	*	*	*	*
4		*	*	*	*	*

* Solubility limit of CHCl_3 exceeded.

Biological properties

Fig. 10a and c show HPLC chromatograms of bile from normal rats collected just before ($t=0$) and 15 min after ($t=15$) intravenous injection of a small bolus (0.25 mg) of either mesobilirubin-III α (**3**) (Fig. 10a) or mesobilirubin-XIII α (**4**) (Fig. 10c) dissolved in rat serum (1 mL). The tallest, most polar, peak in the pre-injection bile ($t=0$) is bilirubin diglucuronide and the two smaller peaks are the two diastereomeric bilirubin monoglucuronides. After injection of **3**, there were marked transient increases in peak area at the retention times of the bilirubin diglucuronide peak and the least polar bilirubin mono-glucuronide peak (Fig. 10a). Similarly, after intravenous injection of **4**, there was a transient increase in peak areas at the retention times of the bilirubin diglucuronide and the most polar bilirubin monoglucuronide peak (Fig. 10c). In neither case were significant quantities of unchanged **3** or **4** detected in bile after their injection. The absorption spectra of the increased peaks were similar to those of the corresponding mesobilirubins III α (**3**) and XIII α (**4**) and were shifted hypsochromically by about 30 nm with respect to the corresponding bilirubin glucuronides. We ascribe the increased peak areas to the diglucuronide and monoglucuronide of the corresponding mesobilirubin isomers, which in our HPLC system do not separate, respectively, from the endogenous bilirubin diglucuronide and one of the monoglucuronides of bilirubin. Consistent with this interpretation, hydrolysis of bile samples collected after injection of mesobilirubins **3** or **4** with NaOH or β -glucuronidase, which is specific for β -glucuronides, resulted in loss of glucuronide peaks and the appearance of both bilirubin and the original mesobilirubins **3** or **4**. To obtain an approximate biliary excretion

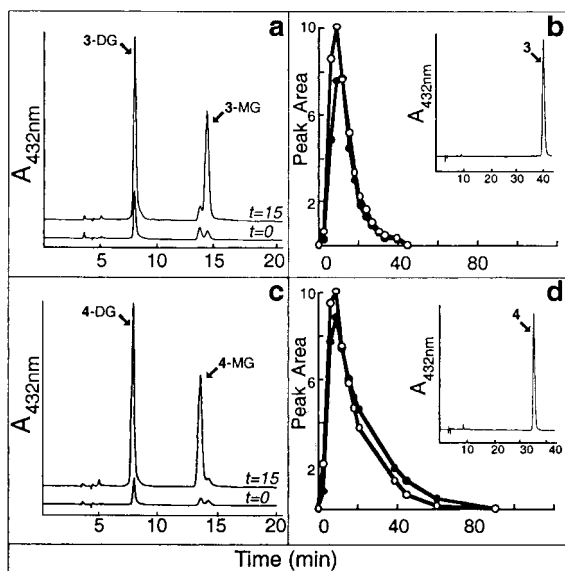


Figure 10. Metabolism of mesobilirubins III α (**3**) and XIII α (**4**) in the rat. Panels **a** and **c** show HPLC chromatograms of bile before ($t=0$) and after ($t=15$ min) injecting 0.25 mg of **3** and **4**, respectively, intravenously into a Sprague-Dawley rat. The $t=0$ chromatograms show the presence of bilirubin diglucuronide (near 8 min) and its two regio-isomeric monoglucuronides (near 14 min). The chromatograms shown as insets in panels **b** and **d** are those of the serum solutions of **3** and **4** injected into rats. Panels **b** and **d** show biliary excretion curves for mono and diglucuronides of **3** and **4** plotted as corrected peak area versus time after injection of mesobilirubin. Open circles are monoglucuronides; closed circles, diglucuronides.

profile for the glucuronides of **3** and **4**, we measured the sum of the peak areas for the bilirubin and mesobilirubin diglucuronides and the sum of the peak areas for the bilirubin and mesobilirubin monoglucuronides and then subtracted from these the estimated contributions from the endogenous bilirubin mono and diglucuronides based on analyses of bile obtained before injection of the mesobilirubins and after elimination of their glucuronides in bile was complete. These biliary excretion profiles are shown in Fig. 10b and d. When **3** or **4** was injected under similar conditions into homozygous Gunn rats, which are mutants that lack bilirubin glucuronidating activity,¹ there was no significant excretion of unchanged compound or yellow metabolites of it in bile over a similar time period. We conclude that exogenous mesobilirubin-III α or XIII α are metabolized in the rat much like endogenous bilirubin. They are not excreted significantly in bile unchanged, but are metabolized to mono and diglucuronides that are excreted promptly in bile, presumably via the MRP-2 (*c*-MOAT) transport system,³⁷ which is thought to mediate the biliary excretion of bilirubin glucuronides. The specific *exo* or *endo* location of the ethyl side-chains does not seem to have a marked effect on their glucuronidation or elimination kinetics.

The two *n*-butyl rubins **1** and **2** are considerably more lipophilic than bilirubin or mesobilirubins-III α and XIII α . Their relative retention times, corrected for dead time, in the methanolic C18 reversed phase HPLC system used for these studies are: mesobilirubin-XIII α , 1.0; bilirubin, \sim 1;

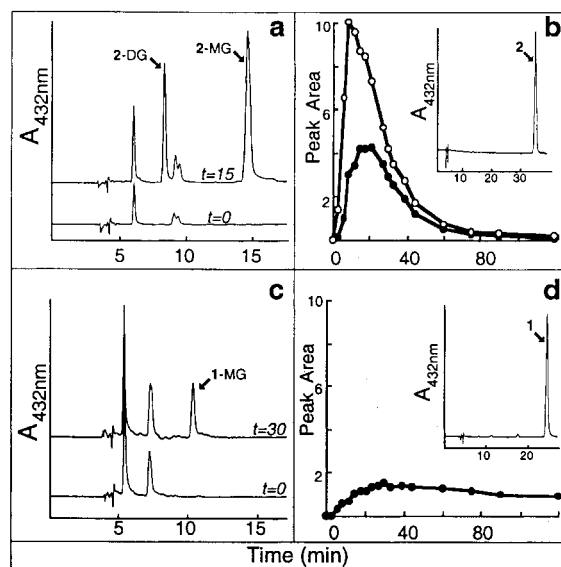


Figure 11. Metabolism and biliary excretion of *n*-butyl rubins **1** and **2** in Sprague-Dawley rats. Panels **a** and **c** show HPLC chromatograms of bile before ($t=0$) and after ($t=15$ or $t=30$ min) intravenous injection of 0.25 mg of **2** or **1**, respectively, into a Sprague-Dawley rat. The $t=0$ chromatograms show the presence of bilirubin diglucuronide and its two monoglucuronides. The solvent system used to generate the chromatograms in panel **c** was slightly different from that used for the HPLCs in panel **a**, and does not resolve the two regio-isomeric monoglucuronides. HPLC chromatograms shown as insets in panels **b** and **d** are of the serum solutions of **2** and **1** injected into the rats. Panel **b** shows biliary excretion curves for the mono and diglucuronides of **2** plotted as HPLC peak area versus time after injection of **2**. Open circles are the monoglucuronide; closed circles, the diglucuronide. Panel **d** shows a biliary excretion curve for the monoglucuronide of **1**.

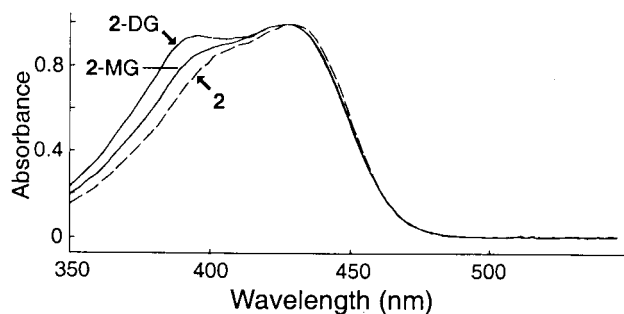


Figure 12. Normalized absorbance spectra of di-*endo* *n*-butyl rubin **2** and its mono and diglucuronides by diode array scanning of the corresponding HPLC chromatogram peaks from bile.

mesobilirubin-III α 1.1; *n*-butyl rubin **1**, 2.2; *n*-butyl rubin **2**, 1.9. After their intravenous injection, they were not excreted in bile in Gunn rats either as metabolites or as intact compounds. In this respect they behave exactly like bilirubin and mesobilirubin. *n*-Butyl rubin **2**, with two *endo* butyl groups, also behaved qualitatively like bilirubin and mesobilirubin in normal Sprague-Dawley rats (Fig. 11a), being excreted as two metabolites that were identified as glucuronides by their susceptibilities to hydrolysis by β -glucuronidase and NaOH. These metabolites were much more lipophilic on HPLC than the corresponding bilirubin glucuronides. The most polar of the two metabolites is, presumably, the diglucuronide of **2**; the less polar, the monoglucuronide. Further evidence for the identity of these peaks as glucuronides of **2** is provided by their absorption spectra (Fig. 12) which are similar to that of **2** but show characteristic shoulders on the short wavelength side of the exciton absorption band. It is noticeable that the ratio of mono to diglucuronide in bile is considerably greater than was observed for the two mesobilirubins **3** and **4**.

The biliary excretion curves for the mono and diglucuronides of **2** (Fig. 11b) are similar to those of **3** and **4**, but broader. This may reflect a lower rate of glucuronidation of **2** and its monoglucuronide relative to the corresponding mesobilirubins. Alternatively, the relatively higher lipophilicity of these organic anions may retard their canalicular secretion into bile.

In contrast to **2**, *n*-butyl rubin **1** (the most lipophilic of the pair, with *exo* *n*-butyl side-chains), was metabolized and excreted very poorly in normal rats. Formation of a single more polar metabolite was observed (Fig. 11c). It is possible that a second metabolite is concealed beneath the endogenous bilirubin mono and diglucuronide peaks, but this seems unlikely since these peaks did not grow following injection of **1** and they retained their spectroscopic integrity. In addition, no additional peak was detected using an HPLC solvent system of higher resolving power. The single metabolite of **1** was identified as a glucuronide (presumably monoglucuronide) on the basis of its absorption spectrum, which resembled that of **1**; by its hydrolysis to **1** by both β -glucuronidase and NaOH; and by its retention time. The concentration of the glucuronide of **1** in bile was low, and the corresponding biliary excretion curve (Fig. 11d) did not show a sharp early peak as the glucuronides of bis-*endo*-*n*-butyl rubin **2** did. The curve was broad, and low concentra-

tions of metabolite were still detectable in bile up to 4 h after injection of **1**. Thus, *n*-butyl rubin **1** and its monoglucuronide metabolite appear to be poor substrates for UGT1A1 or other glucuronosyl transferase enzymes *in vivo*. While it is possible that both mono and diglucuronides are formed, with only the mono being excreted in bile, we think this unlikely because, of the two potential acyl glucuronides, the diglucuronide would be expected to be excreted more rapidly.

Hepatic metabolism

Hepatic uptake followed by intrahepatic glucuronidation is an important route for the detoxification and disposal of compounds bearing COOH, OH, NH and SH groups.^{38,39} Although there has been considerable recent progress in elucidating the primary structures of UDP-glucuronosyl transferases, the chemical mechanisms of enzymic glucuronidation reactions are still unknown. One endogenous compound that commonly undergoes glycosylation in animals is bilirubin, which is metabolized in mammals principally to two isomeric monoglucuronides and a diglucuronide.^{1,2} In the rat these are essentially the only bilirubin metabolites in nascent bile, and unconjugated bilirubin is barely detectable (except as an artifact). Since bilirubin UDP-glucuronosyl transferase has considerable sequence and structural homology to other UDP-glucuronosyl transferases, the chemical mechanisms involved in the glucuronidation of bilirubin are probably similar to those involved in the glucuronidation of other carboxylic acids.

Bilirubin (Fig. 1) has to be glucuronidated for excretion because it is both lipophilic and binds with high affinity to serum albumin and to proteins in the liver. The same is true for mesobilirubins **3** and **4** (Fig. 1), which are not natural products but which behave like bilirubin *in vivo*. Their lipophilicity is thought to stem from a strong tendency to fold into ridge-tile conformations which are stabilized by a web of intramolecular hydrogen bonds. Whether the folded structure is maintained at the glucuronosyl transferase catalytic site is not known, but studies of bilirubin analogs suggest that it is.⁴⁰ Glucuronidation converts the pigment to derivatives that are more polar and more water-soluble and that are excreted expeditiously in bile. The mechanisms by which bilirubin enters hepatocytes and by which the glucuronides find their way into bile are controversial and unclear. The prevailing view is that both processes involve specific transport proteins located in the canalicular membrane.^{37,41} These proteins are thought to be also involved in similar transmembrane transport of a variety of other compounds, particularly organic anions, with little structural resemblance to each other or to bilirubin. If binding to transport proteins is involved, three-dimensional structure and polarity would be expected to be important determinants of hepatic uptake and biliary excretion. However, these factors have received little systematic study.

Homozygous Gunn rats have a metabolic defect that makes them unable to convert bilirubin to its glucuronides.¹ Their bile contains only a very low concentration of unconjugated bilirubin, even after intravenous injection of exogenous

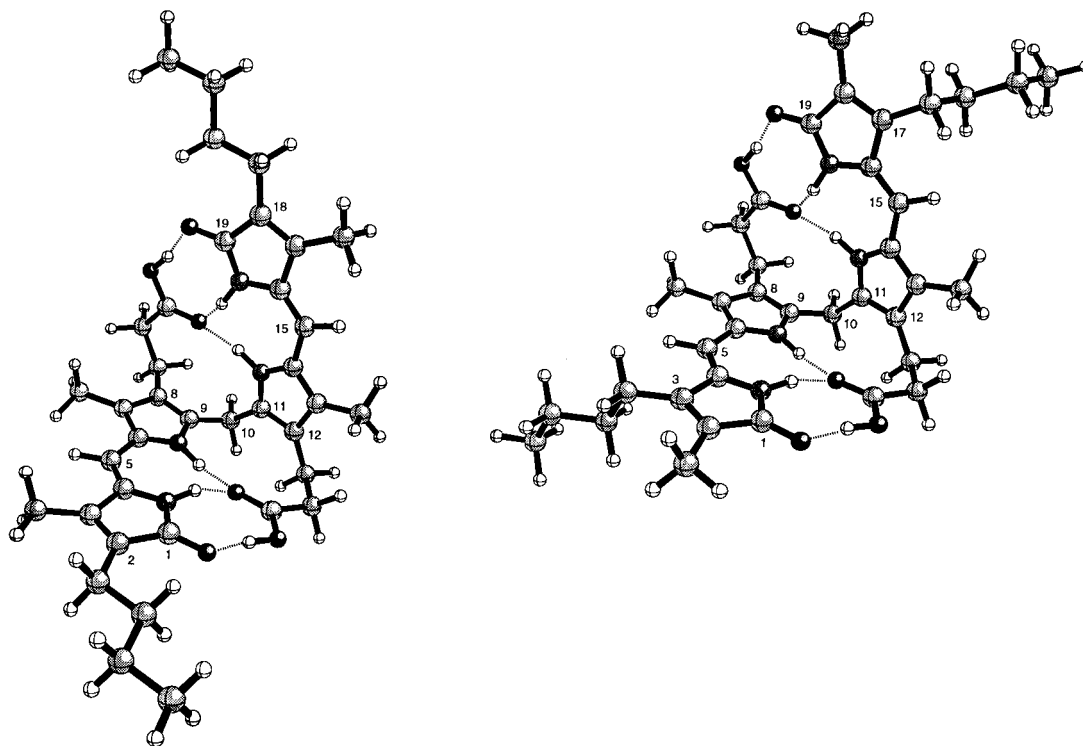


Figure 13. *n*-Butyl rubins **1** (left) and **2** (right) illustrating the greater proximity of the *exo* butyl group of **1** to the lactam carbonyl hydrogen bonding region.

bilirubin. Both **3** and **4** behaved like natural bilirubin when they were administered intravenously to homozygous Gunn rats, as did their *n*-butyl analogs **1** and **2**: none were excreted in bile after injection of small boluses (<1 mg/kg). In contrast, when **2**, **3** or **4** were injected into normal Sprague-Dawley rats, two metabolites, more polar than the parent compound, appeared promptly in bile, along with endogenous bilirubin metabolites (diglucuronide and two isomeric monoglucuronides) as shown by the emergence of strong new peaks on HPLC (Figs. 10a and c and 11a). The concentration of these new metabolites peaked at about 15 min and then slowly dwindled towards zero (Figs. 10b and d and 11b). After ~1–2 h, **2**, **3** or **4** and their metabolites were undetectable in serum. The metabolites had broad double-humped absorption spectra that resembled those of the corresponding parent compound, with similar absorption maxima. On brief treatment of bile with β -glucuronidase, which is specific for β -glucuronides, or with dilute NaOH, the metabolites were converted back to the parent pigments (**2**, **3** or **4**).

In contrast, **1** was excreted very slowly and only as a monoglucuronide in bile in Sprague-Dawley rats. Despite the large difference in lipophilicity between *n*-butyl rubins **1** and **2** and ethyl rubins **3** and **4**, all four compounds appear to be taken up rapidly by the liver from the circulation. Replacing the ethyl groups of **4** with larger *n*-butyl groups has only a weak inhibitory effect on glucuronidation, whereas replacing the two ethyl groups of **3** with *n*-butyls appears to interfere markedly with glucuronidation and biliary excretion. We speculate that bulky groups in the *exo* positions block the access of the lactam carbonyl hydrogen bonding region to a crucial site on the glucuronosyl transferase enzyme.

Concluding comments

In this paper we describe the first high-yield total synthesis, and characterization, of two new lipophilic bilirubin analogs **1** and **2**. The *exo* vs *endo* location of their *n*-butyl groups might not be expected to play a significant role in linear or porphyrin-like conformations, but in the intramolecularly hydrogen-bonded ridge-tile conformation, the *exo*-*n*-butyl acts to shield the lactam hydrogen bonding region (Fig. 13). The *endo*-*n*-butyl is too far removed to exert a similar effect. The studies show that introduction of the *n*-butyl groups can have a marked effect on the polarity of the pigments, making **1** and **2** expectedly less polar (based on HPLC and TLC) than the parent mesobilirubins **3** and **4**. The increased lipophilicity has some effect on the CD spectroscopic properties of **1** and **2**, from which one can discern that presence of an *exo* *n*-butyl appears to interfere with complexation. The energetically most stable conformation of **1** and **2** is still the folded ridge-tile structure preferred by bilirubin and mesobilirubins **3** and **4**. In vivo, the presence of the *n*-butyl groups does not prevent rapid uptake of the compound from blood into the liver or glucuronidation by bilirubin glucuronosyl transferase. However, our experiments show that introduction of the *exo*-butyl group does have a marked effect on the efficiency of glucuronide formation and excretion of **1**.

Experimental

General procedures

All ultraviolet–visible spectra were recorded on a Perkin–Elmer λ -12 spectrophotometer, and all circular dichroism

(CD) spectra were recorded on a Jasco J-600 instrument. Nuclear Magnetic Resonance (NMR) spectra were obtained on a GE QE-300 spectrometer operating at 300 MHz, or on a Varian Unity Plus 500 MHz spectrometer in CDCl₃ solvent (unless otherwise specified). Chemical shifts were reported in δ ppm referenced to the residual CHCl₃ ¹H signal at 7.26 ppm and ¹³C signal at 77.23 ppm. J-modulated spin-echo (Attached Proton Test) and HMQC experiments were used to assign ¹³C NMR spectra. Vapor pressure osmometry measurements were taken on a Gonotec Osmomat 070 osmometer, calibrated with benzil at 45°C in CHCl₃. Melting points were taken on a MelTemp capillary apparatus and are uncorrected. Combustion analyses were carried out by Desert Analytics, Tucson, AZ. Analytical thin layer chromatography was carried out on J.T. Baker silica gel IB-F plates (125 μ m layers). Flash column chromatography was carried out using Woelm silica gel F, thin layer chromatography grade. HPLC analyses were carried out on a Perkin–Elmer Series 4 high performance liquid chromatograph with an LC-95 UV–visible spectrophotometric detector (set at 410 nm) or using an HP-diode array detector (set at 400–450 nm). In either case, the column was a Beckman–Altex ultrasphere-IP 5 μ m C-18 ODS column (25 \times 0.46 cm) fitted with a similarly packed precolumn (4.5 \times 0.46 cm). The flow rate was 0.75–1.0 mL/min; the elution solvent was 0.1 M di-*n*-octylamine acetate in 5–8% aqueous methanol; and the column temperature was \sim 34°C.

Commercial reagents were used as received from Aldrich or Acros, HPLC grade MeOH was from Fisher, β -glucuronidase (*E. coli* Type VII-A, 1000 units/vial), phosphatidyl choline (Type XV-E), cholesterol, taurine, sodium cholate and human serum albumin (defatted) were obtained from Sigma. Spectral data were obtained in spectral grade solvents (Aldrich or Fisher). Homozygous male Gunn rats, weighing 300–400 g, were obtained from our own colony and Sprague-Dawley male rats, weight 370–520 g, were obtained from local commercial vendors. In vivo studies were done in a windowless room under safe lights.

CD and UV measurements

A stock solution of **1**, **2**, **3** or **4** (\sim 7.0 \times 10⁻⁴ M) was prepared by dissolving an appropriate amount of the desired mesobilirubin compound in 2 mL of DMSO. Next, 100 μ L of the stock solution was diluted to 5 mL (volumetric flask) with an HSA solution \sim 2.8 \times 10⁻⁵ M in pH 7.4 Tris buffer. The final concentration of the solution was \sim 1.4 \times 10⁻⁵ M in pigment. Up to seven 5 mL solutions of each pigment were prepared, as needed, in 5 mL volumetric flasks. To each flask was added the indicated volume (μ L) of CHCl₃. Gentle shaking was occasionally required to dissolve all of the CHCl₃ in the aqueous solution, at which point CD and UV–visible measurements were recorded.

1-Nitropentane,⁴² 3-nitro-2-heptanol (**16**)⁴³ and its acetate (**14**)⁴³, 2-nitro-3-heptanol (**17**)⁴⁴ and its acetate (**15**)⁴⁵ were all prepared according to the cited literature, as were 5,5'-diformyl-3,3'-bis(2-ethoxycarbonylethyl)-4,4'-dimethyl-2,2'-dipyrrylmethane (**5**),⁴⁶ 5,5'-di-*tert*-butoxycarbonyl-3,3'-bis(2-ethoxycarbonylethyl)-4,4'-dimethyl-2,2'-dipyrryl-

methane (**18**),⁴⁷ *tert*-butyl 5-acetoxymethyl-4-(2-methoxycarbonylethyl)-3-methyl-1*H*-pyrrole-2-carboxylate (**19**)⁴⁷ and *tert*-butyl 4-(2-methoxycarbonylethyl)-3,5-dimethyl-1*H*-pyrrole-2-carboxylate (**20**).⁴⁸

2-(*p*-Tosyl)-3-methyl-4-*n*-butyl-1*H*-pyrrole (12**).** *p*-Toluene-sulfonylmethyl isocyanide (TosMIC) (17.8 g, 91.28 mmol) was dissolved in 50 mL of 2-propanol–THF (1:1), and had added to it 23.2 g (2.1 mol equiv.) of 1,1,3,3-tetramethylguanidine base (TMG). To the stirred solution was added dropwise 18.5 g (91.33 mmol) of 3-nitro-2-heptyl acetate (**14**) in 50 mL 2-propanol–THF (1:1), and the solution stirred at room temperature for three days. The dark red solution was diluted with 100 mL of CH₂Cl₂, washed with water (3 \times 150 mL) and brine (1 \times 150 mL), dried (anhyd. MgSO₄), filtered and concentrated by rotary evaporation. Hexane was added to crystallize the product, yielding 17.2 g (64.8%) of white crystalline solid. An analytical sample was prepared by the addition of hexane to a CH₂Cl₂ solution of the pyrrole. Colorless crystals were collected and dried over P₂O₅ in an Abderhalden overnight. They had mp 71–72°C and IR (KBr) ν : 2975, 1558, 1459, 1317, 1223, 1141, 1086, 811, 685 cm⁻¹; ¹H NMR δ : 0.93 (3H, t, *J*=7.3 Hz), 1.37–1.27 (2H, m), 1.46–1.39 (2H, m), 2.16 (3H, s), 2.30 (2H, t, *J*=6.8 Hz), 2.38 (3H, s), 6.67 (1H, d, *J*=3 Hz), 7.25 (2H, d, *J*=8 Hz), 7.77 (2H, d, *J*=8 Hz), 9.35 (1H, s) ppm; ¹³C NMR δ : 143.57, 140.52, 129.89, 129.08, 126.79, 124.84, 124.44, 120.28, 32.35, 24.91, 22.63, 21.63, 14.01, 9.34 ppm; MS: *m/z* (relative intensity) 291 [M⁺](44), 248(100), 226(4), 184(4), 156(39), 139(5), 92(10), 65(16) amu. Anal. Calcd for C₁₆H₂₁NO₂S (291.4): C, 65.95; H, 7.26; N, 4.81. Found: C, 66.04; H, 7.24; N, 5.00.

2-(*p*-Tosyl)-3-methyl-4-*n*-butyl-5-bromo-1*H*-pyrrole (10**).** 2-(*p*-Tosyl)-3-methyl-4-*n*-butyl-1*H*-pyrrole (**12**) (0.10 g, 0.34 mmol) was dissolved in 10 mL of CH₂Cl₂ and stirred magnetically in an ice bath. Phenyltrimethylammonium tribromide (0.28 g, 2.2 mol equiv.) dissolved in 50 mL of CH₂Cl₂ was added dropwise, with stirring, over a 10 min period. The solution was stirred for an additional 25 min, then washed with an aqueous sodium bisulfite solution (3 \times 75 mL), water (1 \times 75 mL) and brine (1 \times 75 mL). After drying (anhyd. MgSO₄) and filtration, the solvent was removed by rotary evaporation, yielding 0.12 g white solid (97.2%). An analytical sample was prepared by the addition of hexane to a CH₂Cl₂ solution of the pyrrole. The colorless crystals were collected and dried over P₂O₅ in a drying pistol overnight. They had mp 177–178°C and IR (KBr) ν : 3291, 2953, 2932, 1458, 1365, 1310, 1213, 1164, 1137, 1093, 810, 750, 586 cm⁻¹; ¹H NMR δ : 0.89 (3H, t, *J*=7.3 Hz), 1.40–1.26 (4H, m), 2.16 (3H, s), 2.30 (2H, t, *J*=7.3 Hz), 2.41 (s, 3H), 7.30 (2H, d, *J*=8 Hz), 7.77 (2H, d, *J*=8 Hz), 8.76 (1H, br. s) ppm; ¹³C NMR δ : 143.96, 139.97, 130.04, 126.93, 126.09, 125.59, 104.90, 32.07, 24.73, 22.55, 21.69, 14.01, 9.92 ppm; MS: *m/z* (relative intensity) 371 [M⁺](41), 328(67), 248(100), 135(89), 91(96), 65(30) amu. Anal. Calcd for C₁₆H₂₀NO₂SBr (370.3): C, 51.90; H, 5.43; N, 3.78. Found: C, 51.77; H, 5.47; N, 3.59.

3-*n*-Butyl-4-methyl-5-(*p*-tosyl)-3-pyrrolin-2-one (8**).** Freshly prepared 2-(*p*-tosyl)-3-methyl-4-*n*-butyl-5-bromo-1*H*-pyrrole (**10**) (0.10 g, 0.27 mmol) was dissolved in 5 mL of

TFA followed by 1 mL of water. The dark solution was stirred magnetically overnight at room temperature. The solution was diluted with 15 mL of CH₂Cl₂, washed with water (1×15 mL), saturated aqueous sodium bicarbonate (2×15 mL) and brine (1×15 mL), dried (anhyd. MgSO₄) and filtered. The solution was concentrated (rotary evaporator), and hexane was added to precipitate the product, which was collected by filtration to yield 0.057 g of pure off-white solid (68%). An analytical sample was prepared by crystallization from methanol. It had mp 134–135°C; IR (KBr) ν : 3184, 2952, 2867, 1707, 1597, 1456, 1396, 1312, 1226, 1135, 1083 cm⁻¹; ¹H NMR δ : 0.75 (3H, t, J =6.3 Hz), 0.97–0.91 (4H, m), 2.11–1.92 (2H, m), 2.14 (3H, s), 2.41 (3H, s), 5.02 (1H, s), 6.53 (1H, s), 7.30 (2H, d, J =8.3 Hz), 7.67 (2H, d, J =8.3 Hz) ppm; ¹³C NMR δ 173.06, 146.05, 143.07, 138.59, 130.88, 129.86, 129.68, 79.32, 30.12, 23.29, 22.50, 21.80, 13.98, 13.10 ppm. Anal. Calcd for C₁₆H₂₁NO₃S (291.4): C, 62.52; H, 6.89; N, 4.56. Calcd. for C₁₆H₂₁NO₃S·1/2 CH₃OH (322.4): C, 61.46; H, 7.19; N, 4.34. Found: C, 61.77; H, 7.03; N, 4.29.

3-*n*-Butyl-4-methyl-3-pyrrolin-2-one (6).⁴⁹ 3-*n*-Butyl-4-methyl-5-(*p*-tosyl)-3-pyrrolin-2-one (**8**) (0.100 g, 0.33 mmol) was dissolved in 6 mL of anhydrous ethanol; then to the solution was added 0.0135 g (0.36 nmol) of NaBH₄. The clear solution was stirred at room temperature for 10 min. The NaBH₄ was removed by gravity filtration and the clear solution was washed with dilute acetic acid (1×15 mL), water (2×15 mL) and brine (1×15 mL), extracting each time with CH₂Cl₂. The solvent was removed by rotary evaporation, yielding a white solid (0.045 g, 90.4%). It had mp 89–90°C [lit.⁴⁹ mp 92–3°C]; IR (KBr) ν : 3206, 2950, 1682, 1558, 1540, 1456, 1395 cm⁻¹; ¹H NMR δ : 0.87 (3H, t, J =6.8 Hz), 1.23 (2H, m), 1.39 (2H, m), 1.94 (3H, s), 2.21 (2H, t, J =6.4 Hz), 3.77 (2H, s), 7.94 (1H, s) ppm; ¹³C NMR δ : 176.47, 149.12, 133.05, 80.61, 50.20, 30.81, 23.29, 22.79, 14.01, 13.31 ppm.

Des-2,18-ethyl-2,18-di-*n*-butyl-mesobilirubin-III α (1). 3-*n*-Butyl-4-methyl-3-pyrrolin-2-one (**6**) 0.38 g, 2.45 mmol and 0.15 g (0.37 mmol) of dipyrromethane-dialdehyde (**5**) was dissolved in ~60 mL of methanol and 20 mL of aqueous 6 M KOH. After heating at reflux for 67 h in the dark, the dark brown solution was poured into 150 mL of water (with 30 mg of added ascorbic acid) and cooled in an ice bath. The aqueous solution was acidified with acetic acid, which produced a brown precipitate, and centrifuged. After centrifugation the liquid layers were decanted and the solids filtered (sticky yellow-brown solid). The crude product was then recrystallized from CH₂Cl₂–methanol (three times) to yield a bright yellow solid (0.10 g, 42.7%). It had mp >300°C (dec.); IR (KBr) ν : 3423, 2958, 2860, 1701, 1686, 1637, 1560, 1542, 1439, 1400, 1251, 1166, 1052, 1004, 936 cm⁻¹; ¹H NMR δ : 0.89 (3H, t, J =7.4 Hz), 0.31 (2H, m), 1.44 (2H, m), 2.06 (3H, s), 2.15 (3H, s), 2.29 (2H, t, J =7.6 Hz), 2.56 (1H, ddd, J =16.6, 2.3, 3.4 Hz), 2.79 (1H, ddd, J =19.1, 2.3, 3.4 Hz), 2.88 (1H, ddd, J =14.8, 2.3, 19.1 Hz), 3.01 (1H, ddd, J =14.8, 2.7 Hz), 4.07 (1H, s), 6.04 (1H, s), 9.15 (1H, s), 10.60 (1H, s), 13.65 (1H, br. s). ¹³C NMR δ : 179.73, 174.98, 142.42, 133.32, 129.77, 128.97, 124.37, 123.80, 119.58, 100.77, 32.87, 31.33, 23.36, 22.81, 22.45, 18.79, 14.13, 10.31, 9.91 ppm. Anal. Calcd for

C₃₇H₄₈N₄O₆ (644.8): C, 68.92; H, 7.50; N, 8.69. Found: C, 69.10; H, 7.61; N, 8.51.

2-(*p*-Tosyl)-3-*n*-butyl-4-methyl-1*H*-pyrrole (13). To a solution of *p*-tosylmethyl isocyanide (TosMIC) (11.18 g, 49.23 mmol) and 1,1,3,3-tetramethylguanidine (TMG) (13 mL, 2.1 mol equiv.) in 50 mL of THF–2-propanol (1:1 by vol) was added dropwise over a 1 h period of a solution of 2-nitro-3-heptyl acetate (**15**) (10.0 g, 49.23 nmol) in 50 mL of THF–2-propanol (1:1). The reddish solution was then stirred magnetically for three days. The solution was then diluted with 100 mL of CH₂Cl₂, washed with water (2×100 mL) and brine (1×100 mL), dried (anhyd. MgSO₄) and filtered. Removal of the solvent (rotary evaporator) yielded a honey colored oil. Crystallization from CH₂Cl₂–hexane yielded 14.3 g (75%) of pure product. An analytical sample was prepared by the addition of hexane to a CH₂Cl₂ solution of the pyrrole to afford colorless crystals that were collected and dried over P₂O₅ in a drying pistol overnight. They had mp 85–86°C and IR (KBr) ν : 2955, 1636, 1457, 1307, 1229, 1189, 1144, 1089, 688, 590 cm⁻¹; ¹H NMR δ : 0.87 (3H, t, J =6.3 Hz), 1.31 (4H, m), 1.95 (3H, s), 2.36 (3H, s), 2.58 (2H, t, J =7.3 Hz), 6.68 (1H, d, J =2.4 Hz), 7.23 (2H, d, J =8.3 Hz), 7.78 (2H, d, J =8.3 Hz), 9.60 (1H, br. s) ppm; ¹³C NMR: 143.59, 140.89, 130.05, 129.83, 129.68, 129.10, 126.93, 121.11 ppm; MS: m/z (relative intensity) 291 [M⁺](10), 230(7), 199(7), 136(20), 94(100) amu. Anal. Calcd for C₁₆H₂₁NO₂S (291.4): C, 65.95; H, 7.26; N, 4.81. Found: C, 65.89; H, 7.41; N, 4.80.

2-(*p*-Tosyl)-3-*n*-butyl-4-methyl-5-bromo-1*H*-pyrrole (11). 2-(*p*-Tosyl)-3-butyl-4-methyl-1*H*-pyrrole (**13**) (6.77 g, 23.27 mmol) was dissolved in 50 mL of CH₂Cl₂ and chilled to 0°C in an ice bath. A solution of phenyltrimethylammonium tribromide (PTT) (17.50 g, 46.54 mmol) dissolved in 50 mL CH₂Cl₂ was added dropwise over a 15 min period. After the addition, the solution was stirred magnetically at 0°C for 20 min. The solution was then washed with aqueous sodium bisulfite solution (2×100 mL), water (1×100 mL), and brine (1×100 mL). The solution was then dried (anhyd. MgSO₄), filtered, and the solvent removed (rotary evaporator) to yield 8.61 g (100%) of a light brown solid product that was sufficiently pure for the next step. An analytical sample was prepared by the addition of hexane to a CH₂Cl₂ solution of the pyrrole. The colorless crystals were collected and dried over P₂O₅ in a drying pistol overnight. They had mp 129–130°C and IR(KBr) ν : 3300, 2958, 2859, 1595, 1455, 1371, 1308, 1289, 1204, 1166, 1141, 1110, 814, 715, 699, 652, 588, 526 cm⁻¹; ¹H NMR δ : 0.86 (3H, t, J =7.3 Hz), 1.31–1.22 (4H, m), 1.91 (3H, s), 2.40 (3H, s), 2.55 (2H, t, J =7.8 Hz), 7.29 (2H, d, J =8.3 Hz), 7.76 (2H, d, J =8.3 Hz), 8.86 (1H, br. s) ppm; ¹³C NMR δ : 143.95, 140.10, 130.93, 129.94, 127.00, 124.54, 120.85, 105.37, 32.45, 24.84, 22.95, 21.66, 13.99, 10.01 ppm; MS: m/z (relative intensity) 371 [M⁺](8), 327(8), 214(12), 172(100), 135(16), 91(16) amu. Anal. Calcd for C₁₆H₂₀NO₂SBr (370.3): C, 51.90; H, 5.43; N, 3.78. Found: C, 51.70; H, 5.73; N, 3.62.

3-Methyl-4-*n*-butyl-5-(*p*-tosyl)-3-pyrrolin-2-one (9). Freshly prepared 2-(*p*-tosyl)-3-*n*-butyl-4-methyl-5-bromo-1*H*-pyrrole (**11**) (0.859 g, 2.32 mmol) was dissolved in 20 mL

TFA and had added to it 4 mL water. The dark solution was then stirred magnetically overnight at room temperature. The solution was diluted with 20 mL of CH_2Cl_2 , washed with water (1×50 mL), saturated aqueous sodium bicarbonate (2×50 mL), and brine (1×50 mL), dried (anhyd. MgSO_4), filtered, and the solution concentrated (rotary evaporator). Hexane was added to precipitate the product, which was then filtered to yield 256 mg of pure gray product (36%). It had mp 134–135°C; IR(KBr) ν : 3193, 2960, 2862, 1700, 1597, 1453, 1355, 1318, 1304, 1149, 1084, 809, 749, 668 cm^{-1} ; ^1H NMR δ : 0.95 (3H, t, $J=8.3$ Hz), 1.38 (4H, m), 1.57 (3H, s), 2.42 (3H, s), 2.72 (2H, m), 5.11 (1H, s), 6.28 (1H, s), 7.30 (2H, d, $J=7.8$ Hz), 7.64 (2H, d, $J=7.8$ Hz) ppm; ^{13}C NMR δ : 173.69, 147.93, 145.94, 133.85, 131.06, 129.79, 129.63, 30.78, 26.85, 22.69, 21.80, 13.83, 8.62 ppm. Anal. Calcd for $\text{C}_{16}\text{H}_{21}\text{NO}_3\text{S}$ (291.4): C, 62.52; H, 6.89; N, 4.56. Calcd. for $\text{C}_{16}\text{H}_{21}\text{NO}_3\text{S}\cdot\frac{1}{2}\text{H}_2\text{O}$ (299.4): C, 60.70; H, 6.62; N, 4.65. Found: C, 60.74; H, 7.01; N, 4.43.

3-Methyl-4-*n*-butyl-3-pyrrolin-2-one (7). 3-Methyl-4-butyl-5-(*p*-tosyl)-3-pyrrolin-2-one (**9**) (1.77 g, 5.75 mmol) was dissolved in 50 mL of absolute ethanol which contained a small molar excess of NaBH_4 (240.26 mg). The mixture was stirred magnetically at room temperature for 5 min, then filtered, diluted with 50 mL of CH_2Cl_2 , and washed sequentially with dilute aqueous acetic acid (1×50 mL), water (2×50 mL) and brine (1×50 mL). After drying (anhyd. sodium sulfate) and filtration, a yellow solid was obtained that slowly solidifies upon standing (0.86 g, 74.4%). An analytical sample was prepared by recrystallization from hexane, and the collected crystals were dried over P_2O_5 in a drying pistol overnight. They had mp 110–111°C and IR (KBr) ν : 3269, 2957, 2872, 1771, 1709, 1575, 1351, 1186, 1039, 742, 686 cm^{-1} ; ^1H NMR δ : 0.92 (3H, t, $J=7.3$ Hz), 1.48–1.30 (4H, m), 1.79 (3H, s), 2.36 (2H, t, $J=7.3$ Hz), 3.82 (2H, br. s), 7.09 (1H, br. s); ^{13}C NMR δ : 153.55, 129.88, 48.47, 30.67, 27.88, 22.76, 13.93, 8.51 ppm. Anal. Calcd for $\text{C}_9\text{H}_{15}\text{NO}$ (153.2): C, 70.55; H, 9.87; N, 9.14. Found: C, 70.48; H, 10.05; N, 9.16.

Des-3,17-ethyl-3,17-di-*n*-butyl-mesobilirubin-XIII α (2). 3-Methyl-4-*n*-butyl-3-pyrrolin-2-one (**7**) (0.50 g, 3.26 mmol) and 0.200 g (0.50 nmol) of dipyrromethane-dialdehyde (**5**) was dissolved in ~65 mL of methanol and 20 mL of aqueous 6 M KOH and heated at reflux for 67 h in the dark. The dark brown solution was poured into 150 mL of water (containing 30 mg of ascorbic acid) and cooled in an ice bath. The aqueous solution was acidified with acetic acid, which produced a brown precipitate, and centrifuged. After centrifugation the liquid layers were decanted and the solids filtered (sticky brown/yellow solid). The solid crude product was then recrystallized from CH_2Cl_2 –methanol (two times) yielding a bright yellow solid (0.13 g, 40.1%). It had mp >300°C (dec.) and IR (KBr) ν : 3422, 3259, 2954, 2856, 1701, 1690, 1686, 1677, 1655, 1638, 1619, 1562, 1438, 1400, 1250, 1218, 1180 cm^{-1} ; ^1H NMR δ : 0.91 (3H, t, $J=7.3$ Hz), 1.34 (2H, m), 1.48 (2H, m), 1.86 (3H, s), 2.15 (3H, s), 2.46 (2H, t, $J=7.5$ Hz), 2.56 (1H, ddd, $J=14.8, 3.7, 2.6$ Hz), 2.79 (1H, ddd, $J=18.6, 2.7, 3.7$ Hz), 2.88 (1H, ddd, $J=14.8, 2.6, 18.6$ Hz), 3.01 (1H, ddd, $J=14.5, 14.8, 2.7$ Hz), 4.07 (1H, s), 6.04 (1H, s), 9.15 (1H, s), 10.59 (1H, s), 13.65 (1H, br.s); ^{13}C NMR δ :

179.33, 174.71, 146.90, 133.01, 128.79, 124.07, 123.74, 123.45, 119.31, 100.48, 32.51, 32.36, 24.10, 22.37, 22.09, 18.42, 13.65, 9.86, 7.99 ppm. Anal. Calcd for $\text{C}_{37}\text{H}_{48}\text{N}_4\text{O}_6$ (644.8): C, 68.92; H, 7.50; N, 8.69. Calcd. for $\text{C}_{37}\text{H}_{48}\text{N}_4\text{O}_6\cdot\frac{1}{2}\text{H}_2\text{O}$ (660.8): C, 68.16; H, 7.62; N, 8.48. Found: C, 67.80; H, 7.62; N, 8.40.

Methyl 4-acetyl-5-oxohexanoate. By modifying an earlier procedure for the ethyl ester,⁵⁰ in a 1-L round bottom flask, 30.0 g of KF was dissolved in 200 mL of methanol containing 150 mL of methyl acrylate and 200 mL of 2,4-pentanedione. The flask was fitted with a condenser and stirred at 65°C overnight. The solution was then diluted with ether and washed with water. The ether was removed by rotary evaporator and the excess 2,4-pentanedione removed by distillation under reduced pressure yielding a clear oily product (143.5 g, 71.8%).

Animal studies

The experimental procedures used for studying hepatic metabolism and biliary excretion in Gunn and normal rats are described in detail elsewhere.^{2,40} Briefly, a femoral vein and the common bile duct were cannulated and a liposomal solution containing phosphatidyl choline (1.5 g), cholesterol (62 mg), sodium cholate (12.95 g) and taurine (3.75 g) in 1 L of water was infused (2 mL/h) through the femoral catheter to maintain hydration of the animal and ensure a steady bile flow rate (measured gravimetrically). After the bile flow rate and body temperature had stabilized (~30–60 min), **1**, **2**, **3** or **4** (0.25 mg), dissolved in rat serum (1 mL) with the aid of a small volume (0.1 mL) of DMSO, was infused via the femoral vein as a bolus over a period of about 1 min. Bile was collected in 20 μL aliquots from the tip of the short (5 cm) bile duct cannula immediately before injection of pigment and at frequent intervals thereafter over a period of 4 h. Collection of each sample took about 20 s. Immediately after collection, bile samples were flash frozen in dry ice and then kept at –70°C in the dark until analyzed by HPLC. Blood samples were collected from a small incision in the tip of the tail, allowed to clot, and serum collected by centrifugation was frozen and stored as for bile. For HPLC, bile and serum samples (20 μL) were mixed with 80 μL ice-cold 0.1 M methanolic di-*n*-octylamine acetate (prepared by dissolving equimolar quantities of di-*n*-octylamine and acetic acid in methanol), microfuged for 30 s and 20 μL of the clear supernate was injected onto the column. Biliary excretion curves were derived by plotting HPLC peak areas, determined by integration, against time and are not corrected for small variations in bile flow rate. For hydrolysis of glucuronides with β -glucuronidase, bile (20 μL) was mixed with 40 μL of β -glucuronidase solution (prepared by adding 1 mL of water to one vial of bacterial β -glucuronidase on ice), the mixture incubated for 1 h at 37°C in the dark and then mixed vigorously with 140 μL of 0.1 M di-*n*-octylamine acetate in methanol. This mixture was microfuged for 30–60 s and an aliquot (20 μL) of the supernate was taken for HPLC. For base hydrolysis of glucuronides bile, (20 μL) was mixed with 1 M NaOH (10 μL). After 3 min at room temperature, 10 μL 1 M HCl was added followed, after mixing, by 160 μL of 0.1 M di-*n*-octylamine acetate in methanol. The mixture was vortexed, microfuged for 30–60 s and

an aliquot (20 μ L) of the supernate was taken for HPLC.

Acknowledgements

We thank the National Institutes of Health (HD-17779, DK26307 and GM36633) for support of this research and Ms. Wilma Norona for expert surgical and analytical assistance.

References

1. Chowdhury, J. R.; Wolkoff, A. W.; Chowdhury, N. R.; Arias, I. M. Hereditary Jaundice and Disorders of Bilirubin Metabolism. In *The Metabolic and Molecular Bases of Inherited Disease*, Scriver, C. R., Beaudet, A. L., Sly, W. S., Valle, D., Eds.; McGraw-Hill: New York, 1995; Vol. II, pp 2161–2208.
2. McDonagh, A. F. In *The Porphyrins*, Dolphin, D., Ed.; Academic: New York, 1979; Vol. 6, pp 293–491.
3. Bonnett, R.; Davies, J. E.; Hursthouse, M. B.; Sheldrick, G. M. *Proc. R. Soc. London, Ser. B* **1978**, *202*, 249–268.
4. Person, R. V.; Peterson, B. R.; Lightner, D. A. *J. Am. Chem. Soc.* **1994**, *116*, 42–59.
5. Sheldrick, W. S. *Israel J. Chem.* **1983**, *23*, 155–166.
6. Dörner, T.; Knipp, B.; Lightner, D. A. *Tetrahedron* **1997**, *53*, 2697–2716.
7. Kaplan, D.; Navon, G. *Israel J. Chem.* **1983**, *23*, 177–186.
8. Navon, G.; Frank, S.; Kaplan, D. *J. Chem. Soc., Perkin Trans 2* **1984**, 1145–1149.
9. Trull, F. R.; Franklin, R. W.; Lightner, D. A. *J. Heterocyclic Chem.* **1987**, *24*, 1573–1579.
10. McDonagh, A. F.; Lightner, D. A. In *Hepatic Metabolism and Disposition of Endo and Xenobiotics*; Bock, K. W., Gerok, W., Matern, S., Eds.; Falk Symposium No. 57, Kluwer: Dordrecht, 1991, pp 47–59 (Chapter 5).
11. Trull, F. R.; Person, R. V.; Lightner, D. A. *J. Chem. Soc., Perkin Trans. 2* **1997**, 1241–1250.
12. Shrouf, D. P.; Puzicha, G.; Lightner, D. A. *Synthesis* **1992**, 328–332.
13. Chiefari, J.; Person, R. V.; Lightner, D. A. *Tetrahedron* **1992**, *48*, 5969–5984.
14. Holmes, D. L.; McDonagh, A. F.; Lightner, D. A. *J. Biol. Chem.* **1996**, *271*, 2397–2405.
15. Boiadjev, S. E.; Lightner, D. A. *Synlett.* **1994**, 777–785.
16. Barton, D. H. R.; Kervagoret, J.; Zard, S. Z. *Tetrahedron* **1990**, *46*, 7587–7598.
17. Fischer, H.; Orth, H. *Die Chemie des Pyrrols*; Vol II, first half, Akademische Verlagsgesellschaft, M.B.H., Leipzig 1937.
18. Nogales, D. F.; Ma, J.-S.; Lightner, D. A. *Tetrahedron* **1993**, *49*, 2361–2372.
19. Boiadjev, S. E.; Anstine, D. T.; Lightner, D. A. *J. Am. Chem. Soc.* **1995**, *117*, 8727–8736.
20. Trull, F. R.; Ma, J. S.; Landen, G. L.; Lightner, D. A. *Israel J. Chem.* **1983**, *23*, 211–218.
21. Falk, H. *The Chemistry of Linear Oligopyrroles and Bile Pigments*, Springer: Wien, 1989.
22. Landen, G. L.; Park, Y.-T.; Lightner, D. A. *Tetrahedron* **1983**, *39*, 1893–1907.
23. Boiadjev, S. E.; Anstine, D. T.; Lightner, D. A. *Tetrahedron: Asymmetry* **1994**, *5*, 1945–1964.
24. Holmes, D. L.; Lightner, D. A. *J. Heterocyclic Chem.* **1995**, *32*, 113–121.
25. Boiadjev, S. E.; Pfeiffer, W. P.; Lightner, D. A. *Tetrahedron* **1997**, *53*, 14547–14564.
26. Boiadjev, S. E.; Lightner, D. A. *Tetrahedron: Asymmetry* **1999**, *10*, 2535–2550.
27. Boiadjev, S. E.; Lightner, D. A. *Tetrahedron: Asymmetry* **1997**, *8*, 2115–2129.
28. Kar, A.; Lightner, D. A. *Tetrahedron* **1998**, *54*, 12671–12690.
29. Gawronski, J. K.; Polonski, T.; Lightner, D. A. *Tetrahedron* **1990**, *46*, 8053–8066.
30. Trull, F. R.; Shrouf, D. P.; Lightner, D. A. *Tetrahedron* **1992**, *48*, 8189–8198.
31. Lightner, D. A.; Gawronski, J.; Wijekoon, W. M. D. *J. Am. Chem. Soc.* **1987**, *109*, 6354–6362.
32. Bauman, D.; Killet, C.; Boiadjev, S. E.; Lightner, D. A.; Schönhofer, A.; Kuball, H.-G. *J. Phys. Chem.* **1996**, *100*, 11546–11558.
33. Harada, N.; Nakanishi, K. *Circular Dichroic Spectroscopy—Exciton Coupling in Organic Stereochemistry*, University Science Books, Mill Valley, CA, 1983.
34. Pu, Y.-M.; McDonagh, A. F.; Lightner, D. A. *J. Am. Chem. Soc.* **1993**, *115*, 377–380.
35. Lightner, D. A.; An, J. Y.; Pu, Y. M. *Arch. Biochem. Biophys.* **1988**, *262*, 543–559.
36. Lightner, D. A.; Wijekoon, W. M. D.; Zhang, M.-H. *J. Biol. Chem.* **1988**, *263*, 16669–16676.
37. König, J.; Nies, A. T.; Cui, Y.; Leier, I.; Keppler, D. *Biochem. Biophys. Acta* **1999**, *1461*, 377–394.
38. Burchell, B.; Brierley, C. H. *Bioessays* **1993**, *15*, 749–754.
39. Burchell, B.; Brierley, C. H.; Rance, D. *Life Sci.* **1995**, *57*, 1819–1831.
40. McDonagh, A. F.; Lightner, D. A. *Cell. Mol. Biol.* **1994**, *40*, 965–974.
41. Beier, P. J.; Eckhardt, U.; Schroeder, A.; Hagenbuch, B.; Stieger, B. *Hepatology* **1997**, *26*, 1667–1677.
42. Plummer, C. W.; Drake, N. L. *J. Am. Chem. Soc.* **1954**, *76*, 2720–2721.
43. Sugiyama, T. *Bull. Inst. Chem. Res.* **1989**, *67*, 112–120.
44. Nightingale, D.; James, J. R. *J. Am. Chem. Soc.* **1944**, *66*, 352–354.
45. Carroll, F. I.; White, J. D.; Wall, M. E. *J. Org. Chem.* **1963**, *28*, 1236–1239.
46. Clezy, P. S.; Fookes, C. J. R.; Liepma, A. J. *Austral. J. Chem.* **1972**, *25*, 1979–1990.
47. Mironov, A. F.; Obsepyan, T. R.; Evstigneeva, R. P.; Preobrazhenskii, N. A. *Zh. Obshch. Khim.* **1965**, *35*, 324–328.
48. Smith, K. M.; Pandey, R. K. *J. Heterocyclic Chem.* **1983**, *20*, 1383–1388.
49. Nesvadba, P. PhD Dissertation, Institut für Organische Chemie der Universität Freiburg, Switzerland, 1987.
50. Shrouf, D. P.; Lightner, D. A. *Synthesis* **1990**, 1062–1065.